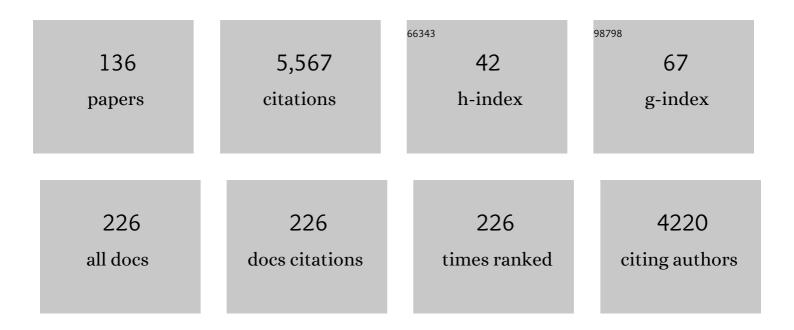
Jacek Lipkowski

List of Publications by Year in descending order

Source: https://exaly.com/author-pdf/693515/publications.pdf Version: 2024-02-01



#	Article	IF	CITATIONS
1	Analyzing Morphological Properties of Early-Stage Toxic Amyloid β Oligomers by Atomic Force Microscopy. Methods in Molecular Biology, 2022, 2402, 227-241.	0.9	2
2	Amyloid β interaction with model cell membranes – What are the toxicity-defining properties of amyloid β?. International Journal of Biological Macromolecules, 2022, 200, 520-531.	7.5	19
3	Effect of Lipid Composition on the Inhibition Mechanism of Amiloride on Alamethicin Ion Channels in Supported Phospholipid Bilayers. Langmuir, 2022, 38, 8398-8406.	3.5	Ο
4	Inhibition of Amyloid β-Induced Lipid Membrane Permeation andÂAmyloid β Aggregation by K162. ACS Chemical Neuroscience, 2021, 12, 531-541.	3.5	14
5	lon transport mechanism in gramicidin A channels formed in floating bilayer lipid membranes supported on gold electrodes. Electrochimica Acta, 2021, 375, 137892.	5.2	12
6	Ion-Pairing Mechanism for the Valinomycin-Mediated Transport of Potassium Ions across Phospholipid Bilayers. Langmuir, 2021, 37, 9613-9621.	3.5	7
7	Mixed monolayer of a nucleolipid and a phospholipid has improved properties for spectroelectrochemical sensing of complementary nucleobases. Journal of Electroanalytical Chemistry, 2021, 896, 115120.	3.8	2
8	Water structure at the multilayers of palladium deposited at nanostructured Au electrodes. Journal of Electroanalytical Chemistry, 2021, 896, 115243.	3.8	2
9	Electrostatics affects formation of Watson-Crick complex between DNA bases in monolayers of nucleolipids deposited at a gold electrode surface. Electrochimica Acta, 2021, 390, 138816.	5.2	3
10	Molecular recognition between guanine and cytosine-functionalized nucleolipid hybrid bilayers supported on gold (111) electrodes. Bioelectrochemistry, 2020, 132, 107416.	4.6	4
11	Water Structure in the Submembrane Region of a Floating Lipid Bilayer: The Effect of an Ion Channel Formation and the Channel Blocker. Langmuir, 2020, 36, 409-418.	3.5	23
12	lonophore properties of valinomycin in the model bilayer lipid membrane 1. Selectivity towards a cation. Journal of Solid State Electrochemistry, 2020, 24, 3125-3134.	2.5	4
13	Alzheimer's disease-related amyloid β peptide causes structural disordering of lipids and changes the electric properties of a floating bilayer lipid membrane. Nanoscale Advances, 2020, 2, 3467-3480.	4.6	17
14	Biomimetics: a new research opportunity for surface electrochemistry. Journal of Solid State Electrochemistry, 2020, 24, 2121-2123.	2.5	5
15	What Vibrational Spectroscopy Tells about Water Structure at the Electrified Palladium–Water Interface. Journal of Physical Chemistry C, 2020, 124, 13240-13248.	3.1	24
16	Spectroelectrochemical studies of structural changes during reduction of oxygen catalyzed by laccase adsorbed on modified carbon nanotubes. Journal of Electroanalytical Chemistry, 2020, 875, 113820.	3.8	6
17	Mechanisms of alamethicin ion channel inhibition by amiloride in zwitterionic tethered lipid bilayers. Journal of Electroanalytical Chemistry, 2019, 848, 113281.	3.8	9
18	Size-Dependent Interaction of Amyloid β Oligomers with Brain Total Lipid Extract Bilayer—Fibrillation Versus Membrane Destruction. Langmuir, 2019, 35, 11940-11949.	3.5	26

#	Article	IF	CITATIONS
19	Electric-Field-Driven Molecular Recognition Reactions of Guanine with 1,2-Dipalmitoyl- <i>sn</i> - <i>glycero</i> -3-cytidine Monolayers Deposited on Gold Electrodes. Langmuir, 2019, 35, 9297-9307.	3.5	8
20	In Situ Electrochemical and PM-IRRAS Studies of Colicin E1 Ion Channels in the Floating Bilayer Lipid Membrane. Langmuir, 2019, 35, 8452-8459.	3.5	10
21	Effects of Amiloride, an Ion Channel Blocker, on Alamethicin Pore Formation in Negatively Charged, Gold-Supported, Phospholipid Bilayers: A Molecular View. Langmuir, 2019, 35, 5060-5068.	3.5	12
22	How Valinomycin Ionophores Enter and Transport K ⁺ across Model Lipid Bilayer Membranes. Langmuir, 2019, 35, 16935-16943.	3.5	33
23	Synthesis and electrochemical characterization of 4-thio pseudo-glycolipids as candidate tethers for lipid bilayer models. Electrochimica Acta, 2019, 298, 150-162.	5.2	5
24	Spectroelectrochemical Characterization of 1,2-Dipalmitoyl- <i>sn</i> -glycero-3-cytidine Diphosphate Nucleolipid Monolayer Supported on Gold (111) Electrode. Langmuir, 2019, 35, 901-910.	3.5	5
25	EIS and PM-IRRAS studies of alamethicin ion channels in a tethered lipid bilayer. Journal of Electroanalytical Chemistry, 2018, 812, 213-220.	3.8	30
26	Role of Transmembrane Potential and Defects on the Permeabilization of Lipid Bilayers by Alamethicin, an Ion-Channel-Forming Peptide. Langmuir, 2018, 34, 6249-6260.	3.5	33
27	Direct visualization of alamethicin ion pores formed in a floating phospholipid membrane supported on a gold electrode surface. Electrochimica Acta, 2018, 267, 195-205.	5.2	31
28	Guided Assembly of Two-Dimensional Arrays of Gold Nanoparticles on a Polycrystalline Gold Electrode for Electrochemical Surface-Enhanced Raman Spectroscopy. Journal of Physical Chemistry C, 2018, 122, 7303-7311.	3.1	5
29	In situ electrochemical and PM-IRRAS studies of alamethicin ion channel formation in model phospholipid bilayers. Journal of Electroanalytical Chemistry, 2018, 819, 251-259.	3.8	23
30	Pore Forming Properties of Alamethicin in Negatively Charged Floating Bilayer Lipid Membranes Supported on Gold Electrodes. Langmuir, 2018, 34, 13754-13765.	3.5	28
31	Electrode-supported biomimetic membranes: An electrochemical and surface science approach for characterizing biological cell membranes. Current Opinion in Electrochemistry, 2018, 12, 60-72.	4.8	31
32	Gramicidin A ion channel formation in model phospholipid bilayers tethered to gold (111) electrode surfaces. Electrochimica Acta, 2017, 243, 364-373.	5.2	23
33	Measurements of surface concentration and charge number per adsorbed molecule for a thiolipid monolayer tethered to the Au(111) surface by a long hydrophilic chain. Journal of Electroanalytical Chemistry, 2017, 793, 203-208.	3.8	7
34	Shell-isolated nanoparticle-enhanced Raman spectroscopy characterization of oxide ores during thiosulfate-mediated gold leaching. Journal of Raman Spectroscopy, 2017, 48, 197-203.	2.5	3
35	Infrared and fluorescence spectroscopic studies of a phospholipid bilayer supported by a soft cationic hydrogel scaffold. Journal of Colloid and Interface Science, 2016, 473, 162-171.	9.4	3
36	Gold Nanorod Arrays: Excitation of Transverse Plasmon Modes and Surface-Enhanced Raman Applications. Journal of Physical Chemistry C, 2016, 120, 16246-16253.	3.1	10

#	Article	IF	CITATIONS
37	Quantitative Subtractively Normalized Interfacial Fourier Transform Infrared Reflection Spectroscopy Study of the Adsorption of Adenine on Au(111) Electrodes. Langmuir, 2016, 32, 3827-3835.	3.5	19
38	Physicochemical Studies on Orientation and Conformation of a New Bacteriocin BacSp222 in a Planar Phospholipid Bilayer. Langmuir, 2016, 32, 5653-5662.	3.5	24
39	Elucidating the interfacial interactions of copper and ammonia with the sulfur passive layer during thiosulfate mediated gold leaching. Electrochimica Acta, 2016, 210, 925-934.	5.2	31
40	Pulsed Potential Dissolution Reduces Anode Residue Formation during Nickel Electroplating. Journal of the Electrochemical Society, 2016, 163, C164-C170.	2.9	2
41	PM-IRRAS Studies of DMPC Bilayers Supported on Au(111) Electrodes Modified with Hydrophilic Monolayers of Thioglucose. Langmuir, 2016, 32, 1791-1798.	3.5	20
42	The Role of Electrochemical Engineering in Our Energy Future. Advances in Electrochemical Science and Engineering, 2015, , 1-6.	0.0	0
43	Electrochemical Shell-Isolated Nanoparticle-Enhanced Raman Spectroscopy: Correlating Structural Information and Adsorption Processes of Pyridine at the Au(hkl) Single Crystal/Solution Interface. Journal of the American Chemical Society, 2015, 137, 2400-2408.	13.7	93
44	SEIRAS Studies of Water Structure in a Sodium Dodecyl Sulfate Film Adsorbed at a Gold Electrode Surface. Langmuir, 2015, 31, 4411-4418.	3.5	20
45	Quantitative SHINERS Analysis of Temporal Changes in the Passive Layer at a Gold Electrode Surface in a Thiosulfate Solution. Analytical Chemistry, 2015, 87, 3791-3799.	6.5	34
46	Infrared and Fluorescence Spectroscopic Investigations of the Acyl Surface Modification of Hydrogel Beads for the Deposition of a Phospholipid Coating. Langmuir, 2015, 31, 11598-11604.	3.5	1
47	Characterization of a Self-Assembled Monolayer of 1-Thio-β-d-Glucose with Electrochemical Surface Enhanced Raman Spectroscopy Using a Nanoparticle Modified Gold Electrode. Langmuir, 2015, 31, 10076-10086.	3.5	19
48	A SERS characterization of the stability of polythionates at the gold–electrolyte interface. Surface Science, 2015, 631, 196-206.	1.9	37
49	Definition of the transfer coefficient in electrochemistry (IUPAC Recommendations 2014). Pure and Applied Chemistry, 2014, 86, 259-262.	1.9	124
50	Defining the transfer coefficient in electrochemistry: An assessment (IUPAC Technical Report). Pure and Applied Chemistry, 2014, 86, 245-258.	1.9	361
51	"Surface-enhanced Raman spectroscopy studies of the passive layer formation in gold leaching from thiosulfate solutions in the presence of cupric ion― Journal of Solid State Electrochemistry, 2014, 18, 1469-1484.	2.5	40
52	Biomimetic Membrane Supported at a Metal Electrode Surface. Behavior Research Methods, 2014, , 1-49.	4.0	12
53	Spectroscopic and Permeation Studies of Phospholipid Bilayers Supported by a Soft Hydrogel Scaffold. Langmuir, 2014, 30, 10862-10870.	3.5	5
54	Molecular resolution visualization of a pore formed by trichogin, an antimicrobial peptide, in a phospholipid matrix. Biochimica Et Biophysica Acta - Biomembranes, 2014, 1838, 3130-3136.	2.6	20

#	Article	IF	CITATIONS
55	Advances in Surface Plasmon Resonance Imaging Enable Quantitative Tracking of Nanoscale Changes in Thickness and Roughness. Analytical Chemistry, 2014, 86, 3346-3354.	6.5	7
56	SEIRAS studies of water structure at the gold electrode surface in the presence of supported lipid bilayer. Journal of Electroanalytical Chemistry, 2014, 716, 112-119.	3.8	56
57	Application of PM-IRRAS to study thin films on industrial and environmental samples. Analytical and Bioanalytical Chemistry, 2013, 405, 1537-1546.	3.7	9
58	Electrochemical SERS study of a biomimetic membrane supported at a nanocavity patterned Ag electrode. Electrochimica Acta, 2013, 110, 120-132.	5.2	27
59	Direct in Situ Observation of Synergism between Cellulolytic Enzymes during the Biodegradation of Crystalline Cellulose Fibers. Langmuir, 2013, 29, 14997-15005.	3.5	36
60	Electrochemical and PM-IRRAS studies of floating lipid bilayers assembled at the Au(111) electrode pre-modified with a hydrophilic monolayer. Journal of Electroanalytical Chemistry, 2013, 688, 76-85.	3.8	22
61	SERS and electrochemical studies of the gold–electrolyte interface under thiosulfate based leaching conditions. Electrochimica Acta, 2013, 111, 390-399.	5.2	51
62	Electrochemical and PM-IRRAS Characterization of Cholera Toxin Binding at a Model Biological Membrane. Langmuir, 2013, 29, 965-976.	3.5	39
63	Biomimetics a New Paradigm for Surface Electrochemistry. Review of Polarography, 2012, 58, 63-65.	0.1	0
64	Direct visualization of the alamethicin pore formed in a planar phospholipid matrix. Proceedings of the National Academy of Sciences of the United States of America, 2012, 109, 21223-21227.	7.1	83
65	Infrared Studies of the Potential Controlled Adsorption of Sodium Dodecyl Sulfate at the Au(111) Electrode Surface. Langmuir, 2012, 28, 2455-2464.	3.5	38
66	Real-Time Observation of the Swelling and Hydrolysis of a Single Crystalline Cellulose Fiber Catalyzed by Cellulase 7B from Trichoderma reesei. Langmuir, 2012, 28, 9664-9672.	3.5	29
67	Non-contact detection of chemical warfare simulant triethyl phosphate using PM-IRRAS. Analytica Chimica Acta, 2012, 737, 45-54.	5.4	6
68	Surface plasmon resonance imaging of the enzymatic degradation of cellulose microfibrils. Analytical Methods, 2012, 4, 3238.	2.7	11
69	Measurements of the Potentials of Zero Free Charge and Zero Total Charge for 1-thio- ± b <i>β</i> -D-glucose and DPTL Modified Au(111) Surface in Different Electrolyte Solutions. Zeitschrift Fur Physikalische Chemie, 2012, 226, 995-1009.	2.8	28
70	2D-SEIRA spectroscopy to highlight conformational changes of the cytochrome c oxidase induced by direct electron transfer. Metallomics, 2011, 3, 619.	2.4	18
71	Atomic Force Microscopy Studies of a Floating-Bilayer Lipid Membrane on a Au(111) Surface Modified with a Hydrophilic Monolayer. Langmuir, 2011, 27, 10867-10877.	3.5	60
72	Electric Field Driven Changes of a Gramicidin Containing Lipid Bilayer Supported on a Au(111) Surface. Langmuir, 2011, 27, 10072-10087.	3.5	44

#	Article	IF	CITATIONS
73	Electrochemical and STM Studies of 1-Thio-β- <scp>d</scp> -glucose Self-Assembled on a Au(111) Electrode Surface. Langmuir, 2011, 27, 13383-13389.	3.5	23
74	Challenges and opportunities of modern electrochemistry—a personal reflection. Journal of Solid State Electrochemistry, 2011, 15, 1673-1677.	2.5	2
75	Building biomimetic membrane at a gold electrode surface. Physical Chemistry Chemical Physics, 2010, 12, 13874.	2.8	94
76	SERS of <i>β</i> â€Thioglucose Adsorbed on Nanostructured Silver Electrodes. ChemPhysChem, 2010, 11, 1460-1467.	2.1	12
77	Direct Visualization of the Enzymatic Digestion of a Single Fiber of Native Cellulose in an Aqueous Environment by Atomic Force Microscopy. Langmuir, 2010, 26, 5007-5013.	3.5	26
78	Quantitative SNIFTIRS studies of (bi)sulfate adsorption at the Pt(111) electrode surface. Physical Chemistry Chemical Physics, 2010, 12, 15231.	2.8	46
79	Potential controlled surface aggregation of surfactants at electrode surfaces – A molecular view. Surface Science, 2009, 603, 1878-1891.	1.9	80
80	In Situ PM-IRRAS Studies of an Archaea Analogue Thiolipid Assembled on a Au(111) Electrode Surface. Langmuir, 2009, 25, 10354-10363.	3.5	67
81	Molecular Resolution Imaging of an Antibiotic Peptide in a Lipid Matrix. Journal of the American Chemical Society, 2009, 131, 6439-6444.	13.7	50
82	Characterizing Changes In The Structure And Orientation Of Supported Model Membranes Upon Binding Of Cholera Toxin B. Biophysical Journal, 2009, 96, 549a.	0.5	0
83	Electric Field Driven Conformational Changes of Gramicidin D in a Model Membrane Supported on a Au(111) Electrode Surface. Biophysical Journal, 2009, 96, 461a.	0.5	0
84	AFM Studies of the Effect of Temperature and Electric Field on the Structure of a DMPCâ^'Cholesterol Bilayer Supported on a Au(111) Electrode Surface. Langmuir, 2009, 25, 1028-1037.	3.5	44
85	Optimization of the parameters for nickel electrowinning using interference microscopy and digital image analysis. Journal of Solid State Electrochemistry, 2008, 12, 453-459.	2.5	6
86	58th Annual meeting of the International Society of Electrochemistry (ISE). Electrochimica Acta, 2008, 53, 6670-6671.	5.2	0
87	AFM Studies of Solid-Supported Lipid Bilayers Formed at a Au(111) Electrode Surface Using Vesicle Fusion and a Combination of Langmuirâ^'Blodgett and Langmuirâ^'Schaefer Techniques. Langmuir, 2008, 24, 10313-10323.	3.5	76
88	STM Studies of Fusion of Cholesterol Suspensions and Mixed 1,2-Dimyristoyl- <i>sn</i> -glycero-3-phosphocholine (DMPC)/Cholesterol Vesicles onto a Au(111) Electrode Surface. Journal of the American Chemical Society, 2008, 130, 5736-5743.	13.7	42
89	Polarization Modulation Infrared Reflectionâ^'Absorption Spectroscopy Studies of the Influence of Perfluorinated Compounds on the Properties of a Model Biological Membrane. Langmuir, 2008, 24, 7408-7412.	3.5	40
90	In Situ STM Study of Potential-Driven Transitions in the Film of a Cationic Surfactant Adsorbed on a Au(111) Electrode Surface. Langmuir, 2007, 23, 12529-12534.	3.5	24

#	Article	IF	CITATIONS
91	Potential-Driven Structural Changes in Langmuirâ d'Blodgett DMPC Bilayers Determined by in situ Spectroelectrochemical PM IRRAS. Langmuir, 2007, 23, 5180-5194.	3.5	107
92	Adsorption ofN-Decyl-N,N,N-trimethylammonium Triflate (DeTATf), a Cationic Surfactant, on the Au(111) Electrode Surface. Langmuir, 2007, 23, 1784-1791.	3.5	27
93	Measurement of the Charge Number Per Adsorbed Molecule and Packing Densities of Self-Assembled Long-Chain Monolayers of Thiols. Langmuir, 2007, 23, 6205-6211.	3.5	68
94	Electric-Field-Driven Surface Aggregation of a Model Zwitterionic Surfactant. Langmuir, 2007, 23, 6937-6946.	3.5	29
95	New Method to Measure Packing Densities of Self-Assembled Thiolipid Monolayers. Langmuir, 2006, 22, 5509-5519.	3.5	73
96	Electrochemical and PM-IRRAS Studies of the Effect of Cholesterol on the Properties of the Headgroup Region of a DMPC Bilayer Supported at a Au(111) Electrode. Journal of Physical Chemistry B, 2006, 110, 26430-26441.	2.6	45
97	Layer-by-Layer PMIRRAS Characterization of DMPC Bilayers Deposited on a Au(111) Electrode Surface. Langmuir, 2006, 22, 10365-10371.	3.5	73
98	Thermodynamic approach to the double layer capacity of a Pt(111) electrode in perchloric acid solutions. Electrochimica Acta, 2006, 51, 3787-3793.	5.2	78
99	Application of atomic force microscopy and scaling analysis of images to predict the effect of current density, temperature and leveling agent on the morphology of electrolytically produced copper. Electrochimica Acta, 2006, 51, 2255-2260.	5.2	16
100	Thermodynamic studies of bromide adsorption at the Pt(111) electrode surface perchloric acid solutions: Comparison with other anions. Journal of Electroanalytical Chemistry, 2006, 591, 149-158.	3.8	52
101	Thermodynamic studies of chloride adsorption at the Pt(111) electrode surface from 0.1 M HClO4 solution. Journal of Electroanalytical Chemistry, 2005, 576, 33-41.	3.8	94
102	In situ IR reflectance absorption spectroscopy studies of the effect of Nafion on CO adsorption and electrooxidation at Pt nanoparticles. Journal of Solid State Electrochemistry, 2005, 9, 267-276.	2.5	15
103	Kinetic Studies of Spreading DMPC Vesicles at the Airâ^'Solution Interface Using Film Pressure Measurements. Langmuir, 2005, 21, 4356-4361.	3.5	18
104	Electrochemical and PM-IRRAS Studies of the Effect of the Static Electric Field on the Structure of the DMPC Bilayer Supported at a Au(111) Electrode Surface. Langmuir, 2005, 21, 330-347.	3.5	100
105	Electrochemical and PM-IRRAS Studies of the Effect of Cholesterol on the Structure of a DMPC Bilayer Supported at an Au (111) Electrode Surface, Part 1: Properties of the Acyl Chains. Biophysical Journal, 2005, 89, 592-604.	0.5	50
106	Adsorption of N-dodecyl-N,N-dimethyl-3-ammonio-1-propanesulfonate (DDAPS), a model zwitterionic surfactant, on the Au(111) electrode surface. Journal of Solid State Electrochemistry, 2004, 8, 693.	2.5	18
107	Self-Assembly of Phospholipid Molecules at a Au(111) Electrode Surface. Journal of the American Chemical Society, 2004, 126, 12276-12277.	13.7	61
108	Layer by Layer Characterization of 1-Octadecanol Films on a Au(111) Electrode Surface. "In Situ― Polarization Modulation Infrared Reflection Absorption Spectroscopy and Electrochemical Studies. Langmuir, 2004, 20, 4579-4589.	3.5	30

#	Article	IF	CITATIONS
109	Determination of the Gibbs excess of H and OH adsorbed at a Pt(111) electrode surface using a thermodynamic method. Journal of Electroanalytical Chemistry, 2003, 558, 19-24.	3.8	60
110	Potential-controlled coordination of coumarin to an Au(210) electrode surface. Journal of Physical Organic Chemistry, 2003, 16, 675-681.	1.9	5
111	PM FTIRRAS Studies of Potential-Controlled Transformations of a Monolayer and a Bilayer of 4-Pentadecylpyridine, a Model Surfactant, Adsorbed on a Au(111) Electrode Surface. Langmuir, 2003, 19, 132-145.	3.5	79
112	In situ Infrared Reflection Absorption Spectroscopy Studies of the Interaction of Nafion® with the Pt Electrode Surface. Zeitschrift Fur Physikalische Chemie, 2003, 217, 513-526.	2.8	34
113	Thermodynamic Studies of Anion Adsorption at Stepped Platinum(hkl) Electrode Surfaces in Sulfuric Acid Solutions. Journal of Physical Chemistry B, 2002, 106, 12787-12796.	2.6	70
114	Electrochemical and PM-IRRAS studies of potential controlled transformations of phospholipid layers on Au(111) electrodes. Faraday Discussions, 2002, 121, 405-422.	3.2	73
115	In situ IR reflectance absorption spectroscopy studies of pyridine adsorption at the Au(110) electrode surface. Journal of Electroanalytical Chemistry, 2002, 524-525, 43-53.	3.8	56
116	Thermodynamic studies of anion adsorption at the Pt(111) electrode surface in sulfuric acid solutions. Journal of Electroanalytical Chemistry, 2002, 534, 79-89.	3.8	98
117	Electrochemical Studies of the Benzoate Adsorption on Au (111) Electrode. Journal of Solution Chemistry, 2000, 29, 987-1005.	1.2	11
118	Reflection FTIR Studies of the Conformation of 2,2â€~-Bipyridine Adsorbed at the Au(111) Electrode/Electrolyte Interface. Langmuir, 2000, 16, 2356-2362.	3.5	38
119	A SNIFTIRS study of the adsorption of pyridine at the Au(111) electrode–solution interface. Electrochimica Acta, 1999, 45, 611-621.	5.2	53
120	1998 Alcan Award Lecture Surface electrochemistry - surface science with a joy stick. Canadian Journal of Chemistry, 1999, 77, 1163-1176.	1.1	13
121	Electrochemical and Spectroscopic Studies of Hydroxide Adsorption at the Au(111) Electrode. Journal of Physical Chemistry B, 1999, 103, 682-691.	2.6	164
122	1998 Alcan Award Lecture Surface electrochemistry - surface science with a joy stick. Canadian Journal of Chemistry, 1999, 77, 1163-1176.	1.1	4
123	Ionic adsorption at the Au(111) electrode. Electrochimica Acta, 1998, 43, 2875-2888.	5.2	192
124	Electroreduction of Hexachlorobenzene in Micellar Aqueous Solutions of Triton-SP 175. Environmental Science & Technology, 1998, 32, 1509-1514.	10.0	21
125	Spectroelectrochemical Investigations of the Spreading of 4â€Pentadecyl Pyridine onto the Au(111) Electrode. Israel Journal of Chemistry, 1997, 37, 197-211.	2.3	26
126	Electrochemical and Raman spectroscopic studies of pyrazine adsorption at the Au(210) electrode surface. Canadian Journal of Chemistry, 1997, 75, 1694-1702.	1.1	8

#	Article	IF	CITATIONS
127	Electrochemical and Fourier Transform Infrared Spectroscopy Studies of Benzonitrile Adsorption at the Au(111) Electrode. Langmuir, 1997, 13, 4737-4747.	3.5	29
128	Prospects for the use of electrochemical methods for the destruction of aromatic organochlorine wastes. Chemosphere, 1997, 35, 2719-2726.	8.2	43
129	Electrochemical and second harmonic generation study of bromide adsorption at the Au(111) electrode surface. Journal of the Chemical Society, Faraday Transactions, 1996, 92, 3737.	1.7	55
130	Coadsorption of metal atoms and anions: Cu upd in the presence of SO42â^', Clâ^' and Brâ^'. Electrochimica Acta, 1995, 40, 9-15.	5.2	167
131	Determination of the sum of Gibbs excesses of sulfate and bisulfate adsorbed at the Pt(111) electrode surface using chronocoulometry and thermodynamics of the perfectly polarized electrode. Journal of Electroanalytical Chemistry, 1995, 388, 233-237.	3.8	89
132	Electrochemical and second harmonic generation study of SO2â^'4 adsorption at the Au(111) electrode. Journal of Electroanalytical Chemistry, 1995, 396, 115-124.	3.8	79
133	Adsorption of Isoquinoline at the Au(111)-Solution Interface. Langmuir, 1994, 10, 2647-2653.	3.5	13
134	Adsorption of pyrazine at the polycrystalline gold-solution interface. Langmuir, 1989, 5, 466-473.	3.5	26
135	Measurement of Physical Adsorption of Neutral Organic Species at Solid Electrodes. Journal of the Electrochemical Society, 1986, 133, 121-128.	2.9	175
136	Quantitative investigations of adsorption of tert-amyl alcohol at the gold(110)-aqueous solution interface. Langmuir, 1986, 2, 630-638.	3.5	52